PNAS

Supplementary Information for

H3N2 influenza A virus gradually adapts to human-type receptor binding and entry specificity after the start of the 1968 pandemic

Mengying Liu[1], A. Sophie Bakker[1], Yoshiki Narimatsu[2], Frank J.M. van Kuppeveld[1], Henrik Clausen[2], Cornelis A.M. de Haan[1*], Erik de Vries[1*]

Erik de Vries

Email: e.devries@uu.nl

This PDF file includes:

Figures S1 to S3

Tables S1 to S6

Figure S1.

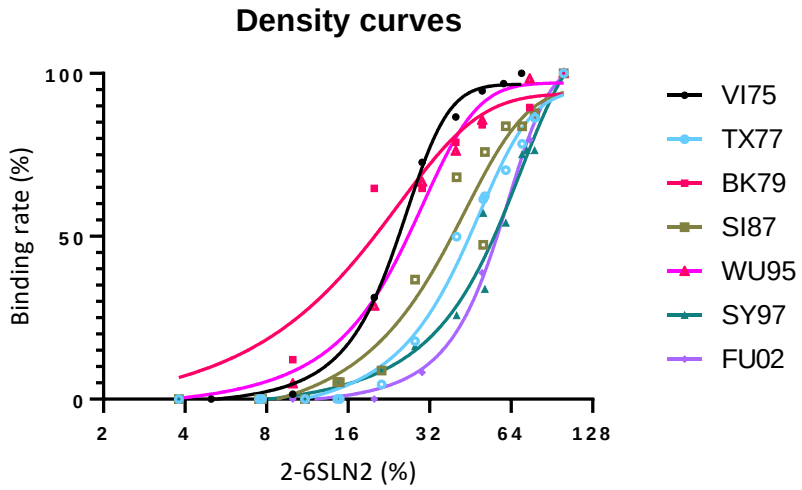

Fig. S1. Effect of receptor density on virus binding rate. Relative virus binding rate (normalized to maximum binding rate per virus) to BLI sensors loaded with different densities of 2-6Sia-(LN)2 was determined for the indicated H3N2 strains and plotted against receptor density. Receptor densities at which binding rate was half-maximal were determined and listed in table S4.

Figure S2.

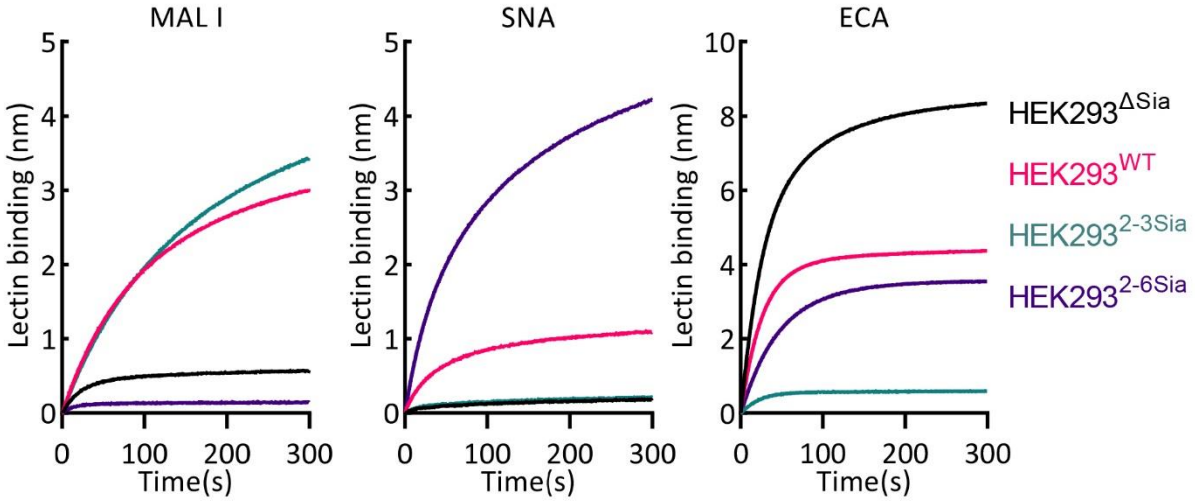

Fig. S2. Lectin binding analysis of LAMP1. Glycan-specific lectins MAL I (terminal Siaα2-3Galβ1-4GlcNAc), SNA (terminal Siaα2-6Galβ1-4GlcNAc) and ECA (terminal Galβ1-4GlcNAc) were associated for 300s to BLI sensors loaded to the same level with LAMP1 produced in the four indicated cell types. A previous study has demonstrated that HEK293$^{2\text{-}6Sia}$ and HEK293$^{2\text{-}3Sia}$ cells transfected with the amounts of ST6Gal1 or ST3Gal4 used here were sialylated to the maximally reachable level [1].

Figure S3.

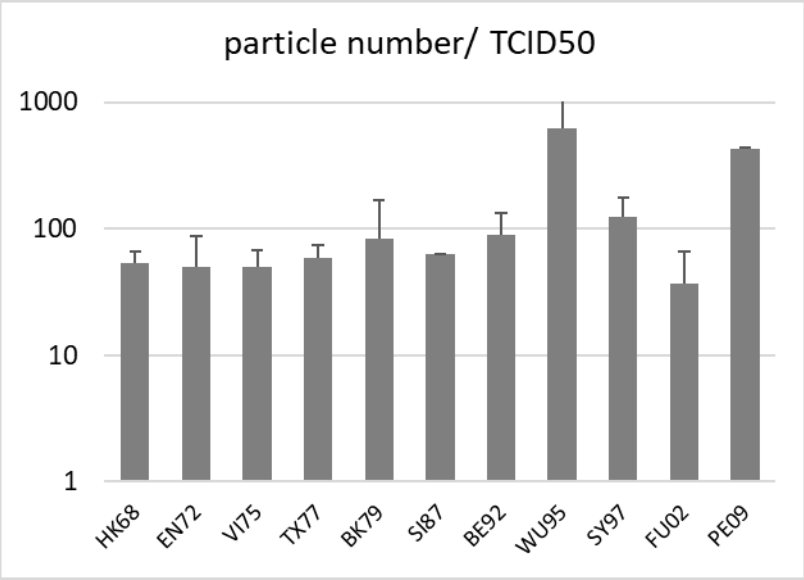

Fig. S3. Infectious titers over virus particle number. Infectious titers were determined by $TCID_{50}$ in duplicate on the 11 H3N2 strains and divided by particle numbers as determined by NTA nano-tracking. Error bars indicate SEM.

Table S1.

Association rate constant of human H3N2 strains

	K_{on} ($M^{-1}min^{-1}$)			
	6SLac	6SLN	3SLac	3SLN
HK68	18277 ± 7082[a]	11597± 7834	9455 ± 5625	12315 ± 10596
EN72	17145 ± 3559	5418 ± 2339	9115 ± 3501	4322 ± 2067
VI75	36301 ± 20452	22904 ± 4978	30425 ± 10273	15460 ± 3609
TX77	49757 ± 15401	19604 ± 8116	14340 ± 4145	5801 ± 1669
BK79	49194 ± 11047	20552 ± 9911	9876 ± 1864	3798 ± 1015
SI87	29577 ± 10170	12206 ± 2983	4566 ± 2213	1444 ± 697
BE92	14024 ± 4540	13697 ± 5269	2137 ± 1001	1176 ± 597
WU95	12116 ± 2356	13461 ± 2376	6235 ± 1829	3743 ± 2177
SI97	3778 ± 3148	4888 ± 2773	1165 ± 496	N.D.[b]
FU02	849 ± 216	3182 ± 1536	N.D.[b]	N.D.[b]
PE09	1613 ± 776	1727 ± 1006	N.D.[b]	N.D.[b]
H5N1 (HU02)	6913 ± 2776	N.D.[b]	49926 ± 10499	19464 ± 10287

[a]Standard deviation

[b]Not determined

6SLac (Siaα2-6Galβ1-4Glc); 6SLN (Siaα2-6Galβ1-4GlcNAc)

3SLac (Siaα2-3Galβ1-4Glc); 3SLN (Siaα2-3Galβ1-4GlcNAc)

Table S2.

Dissociation rate constant of human H3N2 strains

	K_{off} (min^{-1})			
	6SLac	6SLN	3SLac	3SLN
HK68	76.0 ± 6.2[a]	66.8 ± 8.2	69.0 ± 6.9	80.1 ± 9.5
EN72	55.8 ± 3.0	53.4 ± 5.1	73.1 ± 4.5	55.7 ± 5.2
VI75	54.0 ± 5.8	58.2 ± 5.2	55.9 ± 7.9	57.5 ± 4.6
TX77	63.9 ± 6.0	58.9 ± 7.4	54.2 ± 4.2	53.8 ± 4.9
BK79	44.6 ± 3.1	43.2 ± 5.0	55.7 ± 4.2	47.5 ± 3.9
SI87	47.8 ± 3.9	45.5 ± 3.8	53.6 ± 4.4	45.4 ± 4.1
BE92	51.5 ± 4.3	49.9 ± 4.9	46.5 ± 4.5	59.3 ± 6.2
WU95	55.5 ± 3.4	48.0 ± 3.6	52.5 ± 3.7	52.0 ± 5.5
SI97	62.4 ± 9.6	69.3 ± 11.9	47.5 ± 7.8	N.D.[b]
FU02	58.1 ± 2.6	37.7 ± 7.0	N.D.[b]	N.D.[b]
PE09	54.3 ± 9.1	52.9 ± 6.7	N.D.[b]	N.D.[b]
H5N1 (HU02)	49.0 ± 4.9	N.D.[b]	42.3 ± 2.4	39.9 ± 4.4

[a]Standard deviation

[b]Not determined

6SLac (Siaα2-6Galβ1-4Glc); 6SLN (Siaα2-6Galβ1-4GlcNAc)

3SLac (Siaα2-3Galβ1-4Glc); 3SLN (Siaα2-3Galβ1-4GlcNAc)

Table S3.

K_D values determined in this study compared with values reported in literature

		K_D (mM)									
Reference		Sauter [2]	Hanson [3]	Matrosovich [4]	Takemoto [5]	Xiong [6]	Fei [7]		Wang [8]	Ji [9]	Liu
Year of study		1989	1992	1992	1996	2013	2015		2017	2018	this study
Method		NMR	NMR	Endpoint binding[2]	SPR competition	MST	Ellipsometry assoc/dissoc		Endpoint binding[2]	BLI competition	BLI assoc/dissoc
In solution; Surface-bound		HA[1]/glycan	Virus/glycan	Virus/glycan	HA[1]/glycan	recHA$_3$/glycan	Virus/glycan		Virus/glycan	Virus/glycan	Virus/glycan
Temperature		24°C	24°C	4°C	unknown	25°C	15°C	25°C	4°C	20°C	30°C
HK68 or AI68	3SLac	3.2	3.5	2.2	2.4	3.6					7.53
	6SLac	2.1	2.7	2.6	1.2	1.7					4.16
	3SLN					3.13				2.7	6.5
	6SLN					2.03				2.4	5.76
Selectivity ratio	3SLN/6SLN					1.54				1.13	1.13
	3SLac/6Slac	1.52	1.3	0.85	2	2.12					1.81
EN72 or ME71	3SLac						2.6	26.3			8.02
	6SLac						6.8	47.6			3.25
	3SLN										12.89
	6SLN										9.86
Select. Ratio							0.38	0.55			2.47
BE92	3SLac										21.74
	6SLac								1.1		3.67
	3SLN										50.42
	6SLN								1.2		3.64
HU02 or VN04	3SLac					0.7					0.85
	6SLac					21					7.09
	3SLN					1.1					2.05
	6SLN					17					30[3]
Selectivity ratio	3SLN/6SLN					0.06					0.07
	3SLac/6Slac					0.03					0.12

[1]Bromelain-released HA rosettes

[2]Virus coated multi-well plates

[3]For low affinties K_D was estimated by taking half of the projected maximum equilibrium binding level; K_{on} and k_{off} could not be reliably determined from the curves

AI68 (A/Aichi/2/1968(H3N2); ME71 (A/Memphis/1/1971(H3N2)); VN04 (A/Vietnam/1194/2004(H5N1))

Table S4

Relation of K_D to receptor density effects on virus binding under multivalent or heteromultivalent binding conditions

	K_D 6SLN	K_D 3SLN	2-6Sia-(LN)2 density at 50% binding rate	2-6Sia-(LN)2 density at 50% binding rate	K_D 3SLN/K_D 6SLN	50% binding rate Multivalent/Heteromultivalent
			Multivalent[a]	Heteromultivalent[b]		
VI75	2.54	3.72	24.5	17.6	1.5	1.4
TX77	3.01	9.27	45.1			
BK79	2.10	12.50	20.2	10.2	5.9	2.0
SI87	3.73	31.47	38.4			
WU95	3.57	13.88	26.9	13.0	3.9	2.1
SY97	14.17	50[c]	55.2			
FU02	11.85	50[c]	56.2	33.4	4.2	1.7

[a]A density range of 2-6Sia-(LN)2 was complemented by (LN)2 (see Fig. S1)

[b]A density range of 2-6Sia-(LN)2 was complemented by 2-3Sia-(LN)2; values taken from [1]

[c]Approximate K_Ds that could only be estimated from equilibrium binding levels

Table S5.

Statistical analysis of curves fitted to the equation $y=ax^b$ (Fig. 3b-e).

			a					b				
		R^2	a	SE	p	lower 95%	upper 95%	b	SE	p	lower 95%	upper 95%
HEK293^{WT} cells	HK68	1.00	1.58	0.04	6.31E-06	1.49	1.67	1.04	0.01	6.45E-09	1.01	1.07
	EN72	0.99	2.99	0.33	4.97E-04	2.22	4.01	0.77	0.05	9.33E-05	0.63	0.90
	VI75	0.98	10.04	0.34	2.71E-07	9.14	11.02	0.59	0.02	1.64E-05	0.53	0.66
	TX77	1.00	1.17	0.06	3.94E-02	1.01	1.35	0.88	0.03	7.01E-06	0.80	0.96
	BK79	0.96	1.27	0.18	1.47E-01	0.88	1.82	0.95	0.06	8.94E-05	0.79	1.12
	SI87	1.00	0.34	0.02	9.86E-05	0.28	0.41	0.93	0.02	2.54E-06	0.86	0.99
	BE92	0.99	1.37	0.11	1.02E-02	1.12	1.68	1.05	0.05	3.91E-06	0.93	1.18
	WU95	1.00	0.57	0.06	6.07E-03	0.42	0.76	1.04	0.06	5.05E-05	0.89	1.20
	SY97	0.99	0.39	0.05	5.15E-04	0.29	0.53	1.07	0.05	3.96E-06	0.95	1.20
	FU02	0.97	2.96	0.28	2.79E-04	2.30	3.81	1.03	0.07	1.06E-04	0.85	1.22
	PE09	0.99	2.07	0.10	2.18E-05	1.83	2.34	0.97	0.03	2.64E-07	0.90	1.03
HEK293$^{\Delta Sia}$ cells	HK68	1.00	0.0066	0.0009	2.24E-06	0.00	0.01	1.06	0.05	3.31E-05	0.92	1.20
	EN72	0.92	0.0029	0.0005	3.27E-07	0.00	0.00	0.94	0.08	8.30E-05	0.73	1.14
	VI75	0.99	0.0049	0.0006	9.42E-08	0.00	0.01	0.88	0.07	4.27E-05	0.71	1.06
	TX77	0.97	0.0011	0.0003	1.33E-05	0.00	0.00	1.12	0.09	2.25E-04	0.87	1.37
	BK79	0.99	0.0019	0.0008	3.28E-04	0.00	0.01	1.07	0.14	4.42E-03	0.63	1.51
	SI87	0.99	0.0005	0.0002	2.60E-04	0.00	0.00	1.07	0.15	5.53E-03	0.60	1.55
	BE92	0.96	0.0012	0.0004	5.83E-07	0.00	0.00	1.08	0.15	4.12E-04	0.71	1.46
	WU95	0.99	0.0008	0.0002	9.02E-06	0.00	0.00	1.17	0.10	3.19E-04	0.89	1.45
	SY97	0.99	0.0086	0.0020	2.74E-06	0.01	0.01	1.10	0.09	5.37E-05	0.87	1.32
	FU02	0.99	0.0383	0.0037	3.79E-06	0.03	0.05	0.94	0.04	1.78E-05	0.84	1.05
	PE09	0.93	0.1216	0.0269	1.32E-04	0.07	0.20	0.91	0.08	1.19E-04	0.70	1.13
HEK293$^{2\text{-}3Sia}$ cells	HK68	1.00	3.0880	0.2779	4.65E-05	2.47	3.85	0.71	0.04	8.98E-06	0.61	0.80
	EN72	0.99	4.8175	0.3651	2.76E-05	3.93	5.90	0.64	0.06	3.85E-04	0.48	0.80
	VI75	0.98	1.0715	0.0688	3.18E-01	0.91	1.26	0.71	0.03	1.68E-06	0.64	0.78
	TX77	1.00	0.4420	0.0595	2.95E-03	0.31	0.63	0.89	0.09	6.79E-04	0.63	1.14
	BK79	0.96	0.0259	0.0029	4.00E-07	0.02	0.03	1.22	0.05	2.59E-06	1.09	1.35
	SI87	1.00	0.0009	0.0002	2.05E-07	0.00	0.00	1.19	0.08	3.19E-05	0.97	1.41
	BE92	0.99	0.0014	0.0006	9.44E-06	0.00	0.00	1.37	0.17	5.28E-04	0.93	1.82
	WU95	1.00	0.0047	0.0017	1.22E-05	0.00	0.01	1.23	0.14	2.73E-04	0.88	1.58
	SY97	0.99	0.0332	0.0028	2.97E-05	0.03	0.04	1.09	0.05	2.30E-04	0.93	1.25
	FU02	0.97	0.7719	0.1021	9.17E-02	0.56	1.06	0.88	0.06	2.08E-05	0.73	1.03
	PE09	0.99	1.8800	0.1900	1.24E-03	1.47	2.41	0.91	0.04	3.50E-06	0.80	1.01
HEK293$^{2\text{-}6Sia}$ cells	HK68	1.00	2.09	0.06	1.32E-04	1.91	2.30	0.68	0.03	1.45E-04	0.60	0.77
	EN72	0.99	6.73	1.02	1.73E-04	4.55	9.96	0.69	0.11	3.35E-03	0.39	1.00
	VI75	0.98	1.72	0.15	1.15E-03	1.40	2.13	0.66	0.05	3.08E-05	0.54	0.78
	TX77	1.00	3.76	0.35	1.19E-04	2.93	4.81	0.65	0.07	5.70E-04	0.47	0.83
	BK79	0.96	11.79	0.71	1.39E-07	10.15	13.70	0.50	0.04	3.49E-05	0.41	0.59
	SI87	1.00	3.79	0.39	3.91E-05	2.95	4.88	0.76	0.06	5.07E-05	0.61	0.91
	BE92	0.99	8.04	0.77	3.12E-06	6.35	10.18	0.62	0.06	1.12E-04	0.47	0.76
	WU95	1.00	2.45	0.31	1.78E-03	1.75	3.42	0.71	0.08	1.11E-03	0.48	0.95
	SY97	0.99	0.27	0.02	2.49E-05	0.23	0.32	1.08	0.04	1.13E-05	0.97	1.19
	FU02	0.97	3.76	0.30	6.99E-05	3.03	4.66	0.42	0.04	6.68E-04	0.30	0.54
	PE09	0.99	3.75	0.31	1.39E-05	3.06	4.59	1.03	0.04	2.29E-06	0.92	1.14

Table S6.

Statistical analysis of curves fitted to the equation $y=ax^b$ (Fig. 4a shows example for BK79).

		HEK293$^{2\text{-}6Sia}$ cells							HEK293$^{2\text{-}3Sia}$ cells						
		R^2	a			b			R^2	a			b		
			a	SE	p	b	SE	p		a	SE	p	b	SE	p
HK68	1	0.99	0.31	0.02	4.9E-04	0.93	0.07	8.5E-04	0.99	1.0669	0.0786	4.3E-01	0.93	0.07	8.5E-04
	2	1.00	0.45	0.02	2.1E-04	0.75	0.03	2.2E-04	1.00	1.4824	0.0400	6.7E-04	0.78	0.03	7.5E-05
	3	0.99	1.22	0.03	4.7E-03	0.60	0.02	1.6E-04	1.00	0.3021	0.0409	2.5E-03	0.85	0.12	6.1E-03
EN72	1	0.89	1.24	0.22	3.3E-01	0.65	0.18	7.1E-02	0.98	1.7102	0.0787	6.9E-03	0.50	0.05	9.7E-03
	2	1.00	2.87	0.06	3.8E-04	0.79	0.02	8.4E-04	1.00	1.7423	0.0549	3.1E-03	0.73	0.03	2.2E-03
	3	0.98	4.15	0.14	5.1E-04	0.42	0.04	7.3E-03	0.85	1.7439	0.2458	5.2E-02	0.62	0.15	5.1E-02
VI75	1	0.98	0.24	0.02	5.7E-04	0.87	0.09	2.2E-03	1.00	0.3378	0.0105	4.9E-05	0.81	0.03	1.0E-04
	2	1.00	0.90	0.03	4.8E-02	0.77	0.03	1.4E-04	0.99	0.3377	0.0135	1.0E-04	0.84	0.04	1.9E-04
TX77	1	1.00	1.19	0.04	3.1E-02	0.92	0.04	2.2E-03	0.95	0.1896	0.0231	4.5E-03	0.92	0.14	1.6E-02
	2	0.98	1.33	0.09	4.4E-02	0.83	0.08	9.3E-03	0.82	0.1035	0.0097	1.4E-03	0.91	0.11	8.4E-03
	3	1.00	1.38	0.03	4.8E-03	0.96	0.03	1.2E-03	0.99	0.1471	0.0324	1.0E-02	0.96	0.25	5.0E-02
BK79	1	0.80	4.03	0.64	2.6E-03	0.52	0.12	2.1E-02	0.92	0.0074	0.0021	2.9E-04	0.90	0.20	1.9E-02
	2	1.00	5.06	0.12	6.6E-06	0.51	0.02	1.0E-04	1.00	0.0123	0.0018	6.4E-05	1.24	0.11	1.3E-03
	3	0.99	2.45	0.15	6.8E-04	0.70	0.05	6.7E-04	0.98	0.0067	0.0009	3.4E-05	1.11	0.10	1.4E-03
SI87	1	0.98	1.02	0.07	7.7E-01	0.74	0.05	5.3E-04	0.98	0.0003	0.0001	2.0E-05	1.29	0.13	2.1E-03
	2	0.99	0.78	0.03	6.2E-03	0.87	0.03	6.3E-05	0.99	0.0003	0.0001	1.6E-05	1.46	0.12	1.1E-03
	3	0.90	2.51	0.28	3.4E-03	0.69	0.08	3.3E-03	0.99	0.0002	0.0001	9.2E-05	1.50	0.22	6.5E-03
BE92	1	0.99	3.10	0.08	2.4E-05	0.73	0.03	9.3E-05	0.87	0.0004	0.0001	9.1E-05	1.06	0.28	3.1E-02
	2	0.99	2.48	0.08	8.2E-05	0.89	0.03	8.8E-05	0.81	0.0007	0.0004	6.1E-04	1.07	0.48	1.1E-01
	3	0.99	2.29	0.16	1.2E-03	0.87	0.07	1.1E-03	0.89	0.0004	0.0002	1.6E-04	1.18	0.33	3.6E-02
WU95	1	0.97	0.19	0.04	2.9E-03	1.03	0.12	3.7E-03	0.96	0.0016	0.0008	4.5E-04	1.59	0.25	8.0E-03
	2	0.89	0.20	0.02	6.7E-04	0.58	0.07	4.0E-03	0.99	0.0026	0.0005	1.1E-03	1.22	0.48	4.7E-02
	3	0.97	0.90	0.14	4.9E-01	0.80	0.09	3.5E-03	0.94	0.0008	0.0006	1.1E-03	1.09	0.14	1.3E-06
	4	0.85	2.30	0.48	2.2E-02	0.54	0.13	2.4E-02	0.91	0.0005	0.0006	1.9E-03	1.56	0.14	1.3E-06
SY97	1	0.93	0.02	0.00	1.3E-06	0.94	0.09	7.6E-05	0.98	0.0125	0.0072	2.3E-04	0.98	0.29	2.1E-03
	2	0.99	0.11	0.01	4.4E-06	0.97	0.06	1.4E-05	0.99	0.0100	0.0036	6.7E-05	1.20	0.25	1.9E-03
	3	0.99	0.13	0.02	4.0E-05	0.99	0.09	1.1E-04	0.97	0.0103	0.0041	8.0E-05	1.08	0.25	2.5E-03
FU02	1	1.00	1.25	0.03	2.6E-03	0.58	0.02	1.5E-04	1.00	0.3411	0.0318	1.2E-03	0.95	0.09	1.7E-03
	2	0.96	1.45	0.10	1.1E-02	0.65	0.06	2.1E-03	1.00	0.2530	0.0125	9.5E-05	1.01	0.05	2.3E-04
	3	1.00	0.69	0.01	1.2E-04	0.52	0.01	4.1E-05	1.00	0.1386	0.0049	1.2E-05	1.22	0.03	4.6E-05
PE09	1	0.99	0.90	0.08	2.8E-01	1.08	0.07	1.3E-04	0.98	0.3776	0.0234	5.1E-04	1.09	0.06	3.7E-04
	2	1.00	1.89	0.12	5.5E-04	1.07	0.05	3.4E-05	1.00	0.7365	0.0459	1.5E-02	1.01	0.06	4.8E-04
	3	0.99	1.14	0.07	9.2E-02	1.03	0.05	3.4E-05	1.00	0.5583	0.0146	1.9E-04	1.00	0.03	3.8E-05

References

1. M. Liu, et al., Human-type sialic acid receptors contribute to avian influenza A virus binding and entry by hetero-multivalent interactions. Nat Commun 13, 4054 (2022).

2. N. K. Sauter, et al., Hemagglutinins from two influenza virus variants bind to sialic acid derivatives with millimolar dissociation constants: a 500-MHz proton nuclear magnetic resonance study. Biochemistry 28, 8388–8396 (1989).

3. J. E. Hanson, N. K. Sauter, J. J. Skehel, D. C. Wiley, Proton nuclear magnetic resonance studies of the binding of sialosides to intact influenza virus. Virology 189, 525–533 (1992).

4. A. S. Gambaryan, M. N. Matrosovich, A solid-phase enzyme-linked assay for influenza virus receptor-binding activity. J Virol Methods 39, 111–123 (1992).

5. D. K. Takemoto, J. J. Skehel, D. C. Wiley, A surface plasmon resonance assay for the binding of influenza virus hemagglutinin to its sialic acid receptor. Virology 217, 452–458 (1996).

6. S. G. Vachieri, et al., Receptor binding by H10 influenza viruses. Nature 511, 475–477 (2014).

7. Y. Fei, et al., Characterization of Receptor Binding Profiles of Influenza A Viruses Using An Ellipsometry-Based Label-Free Glycan Microarray Assay Platform. Biomolecules 5, 1480–1498 (2015).

8. X. Wang, et al., Amino Acids in Hemagglutinin Antigenic Site B Determine Antigenic and Receptor Binding Differences between A(H3N2)v and Ancestral Seasonal H3N2 Influenza Viruses. J Virol 91, e01512-16 (2017).

9. Y. Ji, R. J. Woods, Quantifying Weak Glycan-Protein Interactions Using a Biolayer Interferometry Competition Assay: Applications to ECL Lectin and X-31 Influenza Hemagglutinin. Adv Exp Med Biol 1104, 259–273 (2018).